



Full Length Article

Diffusion-controlled intercalation approach to synthesize the Ti_2AlC MAX phase coatings at low temperature of 550 °CZhenyu Wang^{a,c,1}, Wentao Li^{a,1}, Yingrui Liu^a, Jintao Shuai^{a,c}, Peiling Ke^{a,b,*}, Aiyang Wang^{a,b,c,*}^a Key Laboratory of Marine Materials and Related Technologies, Zhejiang Key Laboratory of Marine Materials and Protective Technologies, Ningbo Institute of Materials Technology and Engineering, Chinese Academy of Sciences, Ningbo 315201, China^b Center of Materials Science and Optoelectronics Engineering, University of Chinese Academy of Science, Beijing 100049, China^c Ningbo Institute of Industrial Technology, Chinese Academy of Sciences, Ningbo 315201, China

ARTICLE INFO

Keywords:

Nano-laminated structures
Diffusion kinetics
MAX phase
Long-time annealing
Intercalation

ABSTRACT

$M_{n+1}AX_n$ (MAX) phase materials have unique nano-laminated structures and exhibit interesting hybrid properties with ceramics and metals. However, high synthesis temperatures, e.g. typically ≥ 700 °C for Ti_2AlC coatings, are the key barriers to their wide application on various substrates. In this study, Ti_2AlC MAX phase coatings were firstly fabricated by annealing the pre-designed $\alpha-TiC_{0.65}/Al$ multilayer coatings at temperatures as low as 550 °C till now, which is the lowest synthesis temperature compared to already-reported literatures. Different with the common used short-time annealing (1–3 h), noted that the long-time annealing from 15 h to 400 h was particularly conducted based on the sluggish diffusion kinetics at lower temperature. Moreover, the dependence of structural evolution upon annealing proposed that Al diffusion-controlled intercalation process played the key factor to reduce the the formation temperature of Ti_2AlC MAX phase. The results provide a strategy to fabricate high-quality Ti_2AlC MAX phase coatings at 550 °C for wide application of temperature-sensitive substrates.

1. Introduction

$M_{n+1}AX_n$ (MAX) phases are a family of ternary carbide and nitride ceramics with layered hexagonal crystal structure (space group $P6_3/mmc$) [1]. Herein, M is an early transition metal, A is an element primarily from Groups 13 and 14, X is carbon and/or nitrogen, and $n = 1-3$ and possibly higher. Over 70 MAX phases are currently known to exist. Such phases have attracted considerable attention because of their unique structure and corresponding interesting properties [2]. In structure, near-close packed $M_{n+1}X_n$ sheets are interleaved by pure one-atom-thick A-layer. The A-layer can be easily removed from a $M_{n+1}AX_n$ phase through chemical etching, resulting in stand-alone two-dimensional (2D) $M_{n+1}X_n$ sheets known as MXene, which are increasingly stimulated for applications including catalysis, energy storage, electromagnetic wave interference shielding, etc. [3–7]. MAX phases are well-known for their interesting properties as they are a combination of those of ceramics and metals, where these ceramic materials display good electrical and thermal conductivity, high-temperature resistance and damage tolerance, excellent thermal shock resistance, as

well as superior oxidation resistance in air and water vapor, etc. [8–11]. Owing to these hybrid properties, MAX phases are considered to be promising materials for nuclear energy applications and accident tolerance, either as fuel cladding or as coating materials.

In past few years, MAX phases have been fabricated by various kinds of techniques, including bulk synthesis by hot isotactic pressing and thin film deposition [12]. However, owing to their complex crystalline structure with a large unit cell, the growth of bulk MAX phases requires high synthesis temperatures, generally above 1000 °C [13]. As an alternative existence, the MAX phases in nanometer or even atomic scaled thin-film/coatings can be deposited by magnetron sputtering at lower temperature ~ 700 °C. However, it is still impossible to obtain the Ti-based MAX phase coatings with high crystallinity and phase purity as well as dense structure at temperature below 700 °C. This makes the Ti-based MAX phase coatings impossible applications for temperature-sensitive substrates, such as zirconium alloys, steel, titanium alloys, etc. How to fabricate the high-quality Ti_2AlC MAX phase coatings with high performance under 700 °C is still a highly challenging issue.

Reducing the reaction barrier via a special reaction pathway has

* Corresponding authors at: Key Laboratory of Marine Materials and Related Technologies, Zhejiang key Laboratory of marine Materials and Protective Technologies, Ningbo Institute of Materials Technology and Engineering, Chinese Academy of Sciences, Ningbo 315201, China.

E-mail addresses: kepl@nimte.ac.cn (P. Ke), aywang@nimte.ac.cn (A. Wang).

¹ These authors contributed equally to the work.

been demonstrated to effectively decrease the formation temperature of MAX phases. Zhou and Riley et al. [14,15] reported a novel low-temperature synthesis method whereby Si or Al were intercalated into TiC_x ($x < 1$) with hexagonal structure to directly form the MAX phase. By intercalation, the Ti_3AlC_2 MAX phase could be synthesized at a temperature 400–600 °C lower compared to the conventional bulk synthesis temperature. Abdulkadhim et al. [12] verified the intercalation mechanism by annealing treatment of the TiC_x/Al bilayer thin film with combinatorial magnetron sputtering. They found the Ti_2AlC MAX phase was formed at the annealing temperature of 700 °C. However, further lower temperatures were not feasible during annealing because of the requirement of a long diffusion length of Al in the above bilayer films. Apart from these efforts, improving surface diffusion has also been proposed to achieve a lower synthesis temperature during sputtering deposition of crystalline MAX-phase thin films [16]. It is most likely that surface diffusion can reduce the kinetic limitations of deposited atoms, and then promote the atoms involved to reach their proper crystal lattice sites and crystallize by enhanced energetic ion bombardment. Huang and Su et al. [17,18] have reported one-step synthesis of phase-pure V_2AlC and Ti_2AlC films above 600 °C by increasing the sputtered ion flux, provided that a near-stoichiometric V_2AlC and Ti_2AlC composition is required. Although no other competing phases (e.g., intermetallic compound, metal carbide,) were found, the MAX-phase films fabricated in this manner were poorly crystalline, which could cause a significant worse impact on their properties.

Similar to the MAX-phase synthesis process and based on fast surface dynamics, Wang et al. [19] manipulated the sophisticated superlattice-like nanostructure on the surface of $\text{Pd}_{40}\text{Ni}_{10}\text{Cu}_{30}\text{P}_{20}$ metallic glass, where the atoms were arrayed layer by layer in a modulated period of 2.6 nm, by prolonging the annealing time to 100 h at a temperature below the glass transition temperature. In addition, dedicated long-time annealing of metastable Fe-Cr alloy films benefited to form Fe-Cr superstructure multilayers with periods of one or few atomic monolayers of the individual components [20]. Therefore, it could be deduced that surface dynamics played a key role in phase formation with complex crystal structures during the long-time annealing treatment that offered a possible strategy to reduce the phase formation temperature for MAX phases. However, most of current studies on the preparation of MAX-phase coatings by this two-step method, i.e., low-temperature deposition followed by annealing treatment, focused on short-time annealing for 1–3 h [21–23], the effects of long-time annealing on the formation of MAX-phase coatings at low temperature less than 600 °C is lack of study yet.

In order to obtain the MAX phase with high crystallinity at relatively low temperatures, in this work, we manipulated a designed multilayer Ti-Al-C coating with hexagonal TiC_x and Al atomic layers alternately growing along the direction perpendicular to substrate. Subsequently, the as-deposited multilayer Ti-Al-C coatings were subjected to long-time annealing treatment. The formation of the Ti_2AlC MAX phase was observed after annealing at 550 °C for 100 h due to the Al diffusion-controlled intercalation process. The results provide new insights into the relationship between the annealing temperature/time, and the resulted MAX phases at low temperatures, and bring forward a strategy to fabricate other MAX phase coatings for wide applications with temperature-sensitive substrates.

2. Experimental details

2.1. Coating preparation

Multilayer Ti-Al-C coatings were deposited on Ti-6Al-4V (TC4) substrates by a home-made hybrid arc bonded sputtering system, as illustrated in Fig. 1. The nominal composition of the substrates in weight per cent is: Al, 6.04; V, 4.03; Fe, 0.3; O, 0.1; C, 0.1; N, 0.05; H, 0.015 and the balance Ti. A circular titanium target ($\Phi 128$ mm; 99.9% purity) was used as an arc cathode source, and the rectangular

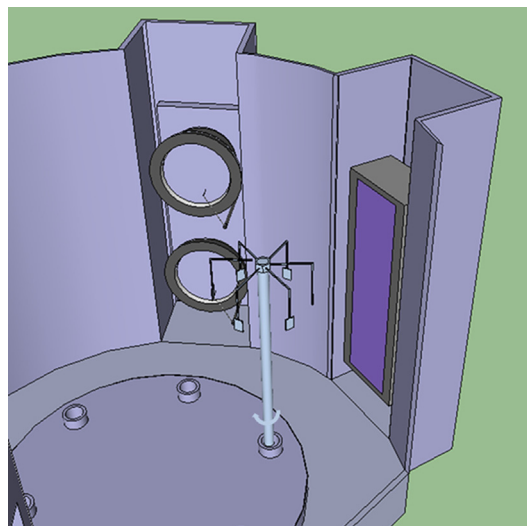


Fig. 1. Schematic diagrams of the coating deposition system, where the circular titanium target and rectangular aluminum target were used.

aluminum target (400 mm × 100 mm × 7 mm; 99.9% purity) was used for the sputtering source. Gas mixtures of Ar (99.999%) and CH_4 (99.99%) were used as reactive gas sources, and the flow rates of Ar and CH_4 were kept at 200 sccm and 15 sccm, respectively, with the chamber pressure of 2.0 Pa. To improve the adhesion strength, glow discharge cleaning was conducted and TiN diffusion barrier of ~600 nm was set prior to deposition. During deposition, the arc power to the Ti target and the sputter power to the Al target were controlled at 18 W and 3.1 kW, respectively. The DC negative bias voltage of -200 V was applied to the substrates without any other intentional heating. After 90 min deposition, the total thickness of the as-deposited multilayer Ti-Al-C coatings was about 7 μm . The modulation period and ratio of the TiC_x and Al layer were controlled at ~20 nm and 2:1, respectively, by adjusting the sample rotation rate.

2.2. Annealing treatment, chemical composition and structural analysis

Isothermal annealing treatment was conducted in a tube furnace. Before the annealing process, the furnace was pumped down to 1.0×10^{-2} Pa and then Ar was introduced immediately until the pressure was 1×10^5 Pa. Thereafter, the tube furnace was heated to the annealing temperature at a heating rate of $\sim 4 \text{ K min}^{-1}$ under the flowing Ar atmosphere. The chemical composition of as-deposited coating was tested by Rutherford backscattering spectrometry (RBS), which was performed with a 2.0 MeV ^4He on the coating at 160° angle. The data fitting by SIMNRA software established that atomic ratio of Ti, Al, C and O was determined to be 1:0.31:0.65:0.11, as it is shown in Fig. 2. The O contaminant was also found in the as-deposited coating, probably resulting from low vacuum degree during deposition process. For the energy calibration of each channel, high purity Cu plates, Au films were employed. Structural analysis was carried out by X-ray diffraction (XRD), with a BrukerD8 Advance diffractometer, using $\text{Cu K}\alpha$ radiation. Cross-sectional transmission electron microscopy (XTEM) specimens were prepared with a focused ion beam (FIB) equipment (Auriga, Zeiss). Details of cross sectional TEM sample preparation using FIB are given in Ref. [24]. XTEM, high-resolution transmission electron microscopy (HRTEM), scanning transmission electron microscopy (STEM) and high-angle annular dark-field (HAADF)-STEM studies were performed on a FEI Tecnai F20 system.

3. Results and discussion

The reaction pathway between $\text{TiC}_{0.65}$ ($x < 1$) and Al can reduce

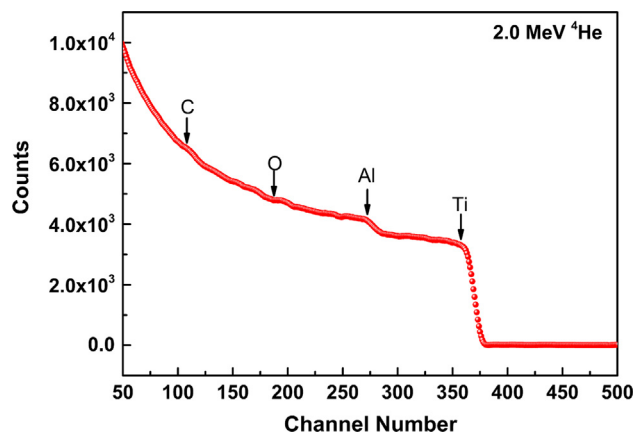


Fig. 2. RBS spectra on as-deposited multilayer Ti-Al-C coatings at 160° angle.

the reaction barrier for the formation of Ti_2AlC MAX phases. As expected, multilayer Ti-Al-C coatings were successfully deposited using arc bonded sputtering technology in this study, as shown in Fig. 3. A schematic diagram of the pre-designed multilayer Ti-Al-C coating was illustrated in Fig. 3a. From the TEM bright-field image (Fig. 3b), the layered structure was well defined with the dark and bright layer thicknesses of ~ 15 nm and ~ 7 nm, respectively. Because of the higher electron scattering factor for Ti atoms, Ti-containing layers displayed a darker contrast than the Al-containing layer in the bright-field image. Fig. 3c presented the selective area electron diffraction (SAED) pattern of the as-deposited Ti-Al-C coatings, which were characterized by polycrystalline α -Ti phases with a hexagonal structure and a TiC phase with face centered cubic structure. The solubility of light elements such

as C was generally high in α -Ti [25]; it was found that C existed in conjunction with the Ti element as a strong carbide-forming element. Thus, it was concluded that C mainly existed in the Ti-containing layer. The filtered inverse fast Fourier transformation (IFFT) image (Fig. 3e) and the fast Fourier transformation (FFT) image (Fig. 3f) of the square region marked in Fig. 3d showed the single-phase hexagonal α -Ti structure, which was consistent with the SAED results. The IFFT image also clearly showed that the Al partially exhibited continuous lattice fringes with α -Ti layer, which were induced by the strong texture template effects of the α -Ti layer.

The HAADF-STEM cross-sectional image of the as-deposited multilayer Ti-Al-C coatings, along with the corresponding EDS results, was presented in Fig. 4. The HAADF-STEM image (Fig. 4a) revealed a well-defined nanoscaled-layered structure with alternate bright and dark layers due to different average atomic numbers. The EDS mapping results from the square region, as illustrated in Fig. 4b, showed that the Ti and Al layers grew alternately with the period modulation of ~ 22 nm. Additionally, C element was mainly present in the Ti layer, either dissolved in the Ti lattice or bonded with Ti. The EDS line scanning along the yellow line was shown in Fig. 4c. Although absolute quantification is not precise because of the limited resolution of EDS, the Ti, Al, and C line profiles clearly indicated that most of the C was stored in the Ti layers.

HRTEM and STEM were employed to examine the cross-section microstructure of the Ti-Al-C coatings after 100 h annealing at 550°C . Fig. 5 showed the cross-sectional view of the annealed coatings. After 100 h annealing, the initial multilayer structure disappeared because of the interdiffusion of low-melting Al. The typical stacking sequence for the Ti_2AlC phase with two TiC-slabs interleaved with a square-planar layer of Al could be seen in the HRTEM image (Fig. 5b and d), with the electron beam parallel to the $[11\bar{2}0]$ direction. The c lattice parameter

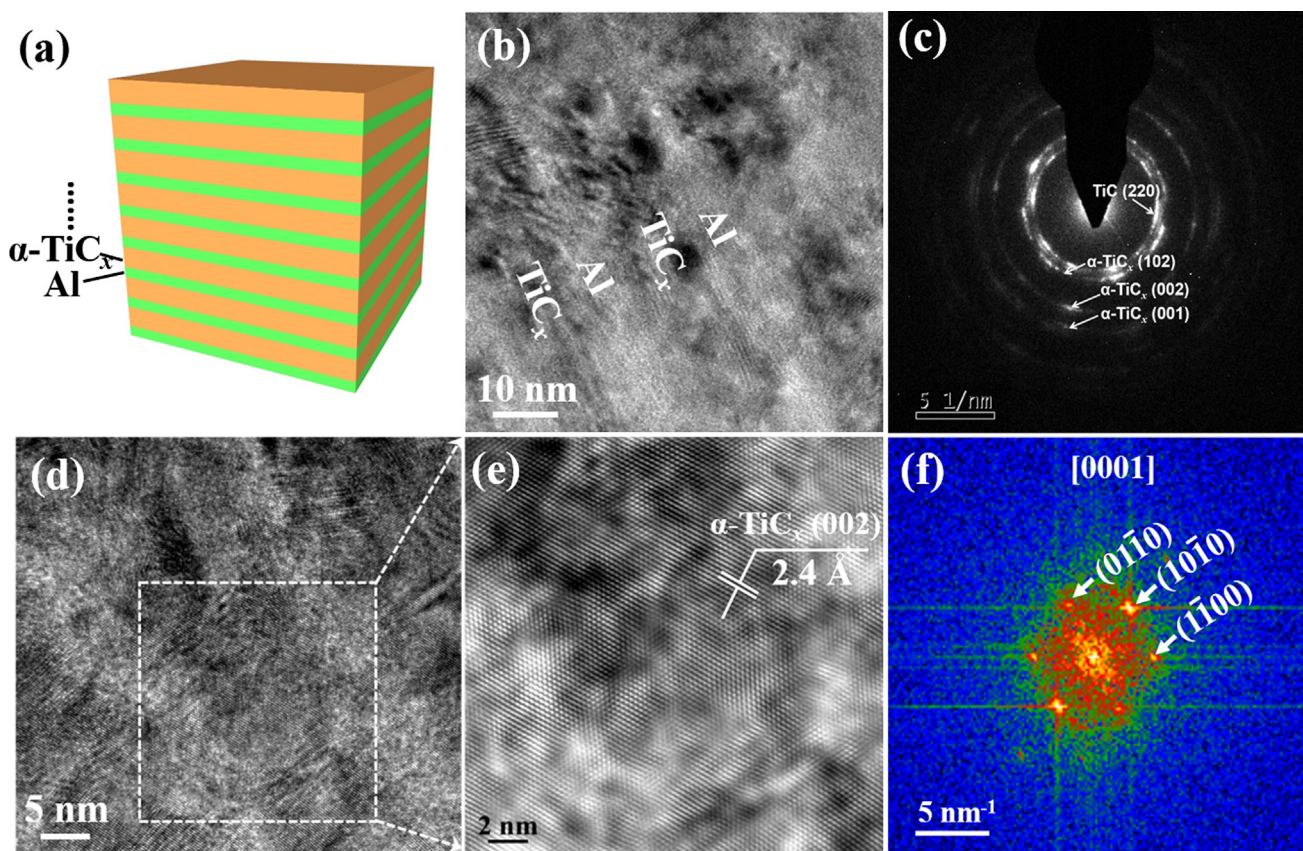


Fig. 3. Microstructures of the as-deposited multilayer Ti-Al-C coatings. (a) Schematic diagram of the pre-designed Ti-Al-C multilayer coating. (b) Low-magnification TEM images of as-deposited Ti-Al-C multilayer coating. (c) SAED patterns of the as-deposited Ti-Al-C coatings. (d) HRTEM. (e) Enlarged view of the local areas selected in (d). (f) FFT image after periodic filtering processing from the marked areas in (c).

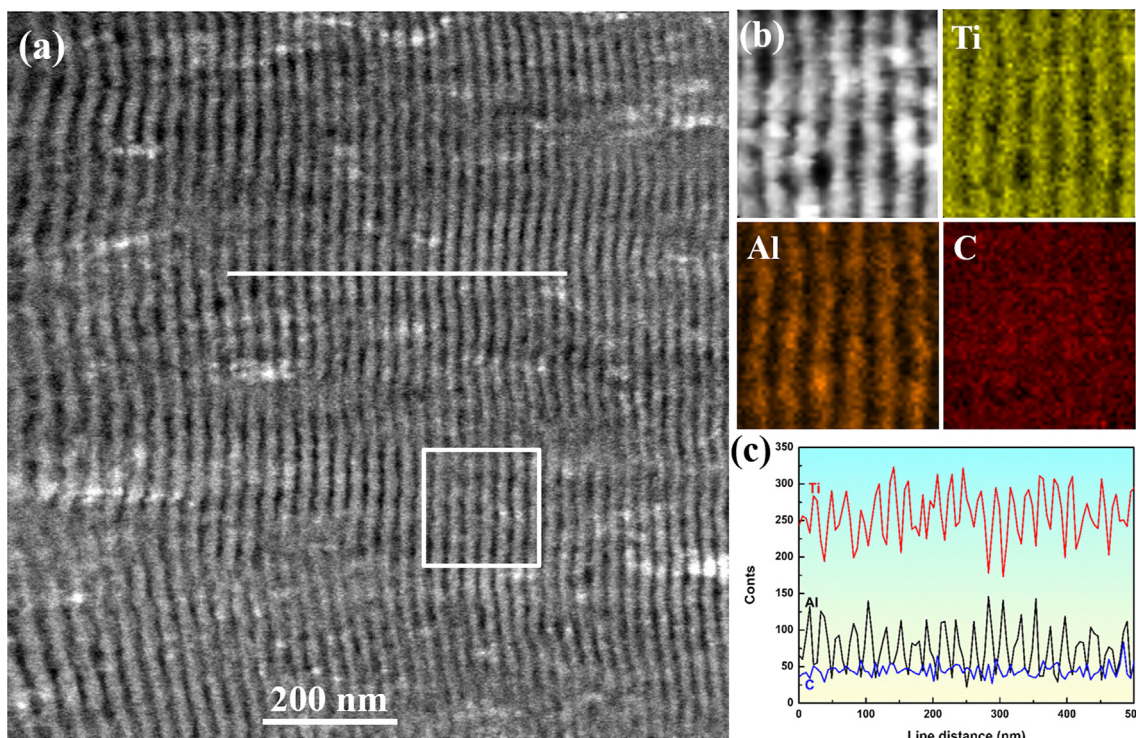


Fig. 4. (a) STEM image of the as-deposited multilayer Ti-Al-C coatings. (b) EDS mapping and (c) EDS line-scanning of the yellow square area and line labeled in (a).

deduced from the enlarged HRTEM image, as shown in Fig. 5e, was 1.36 nm, a value that was in good accordance with the previous measurement [26]. A typical FFT image corresponding to the Fig. 5e was shown in Fig. 5f. The typical (0 0 0 l) spots of the MAX phase could be clearly identified in this FFT image. Fig. 5c showed HRTEM images with two distinctively different regions (indicated with “A” and “B”, see insert in Fig. 5c, namely, phases “A” and “B”, which were identified as Ti_2AlC and TiC_x (0 0 2), respectively, with TiC_x being epitaxial to the

Ti_2AlC phase. This suggested that the Ti_2AlC MAX phase was not formed by nucleation and growth, but instead Al intercalated into TiC_x and led to MAX phase formation, similar to previous observations and discussions in Refs. [14,15,27]. The $\alpha-TiC_x$ phase had the same hexagonal close-packed (*hcp*) crystal structure as the Ti_2AlC MAX phase, which implied that Ti_2AlC transformation was likely enabled by the very short diffusion distance, as a majority of the atomic planes of Ti remaining unchanged [28]. Hence, the formation temperature for

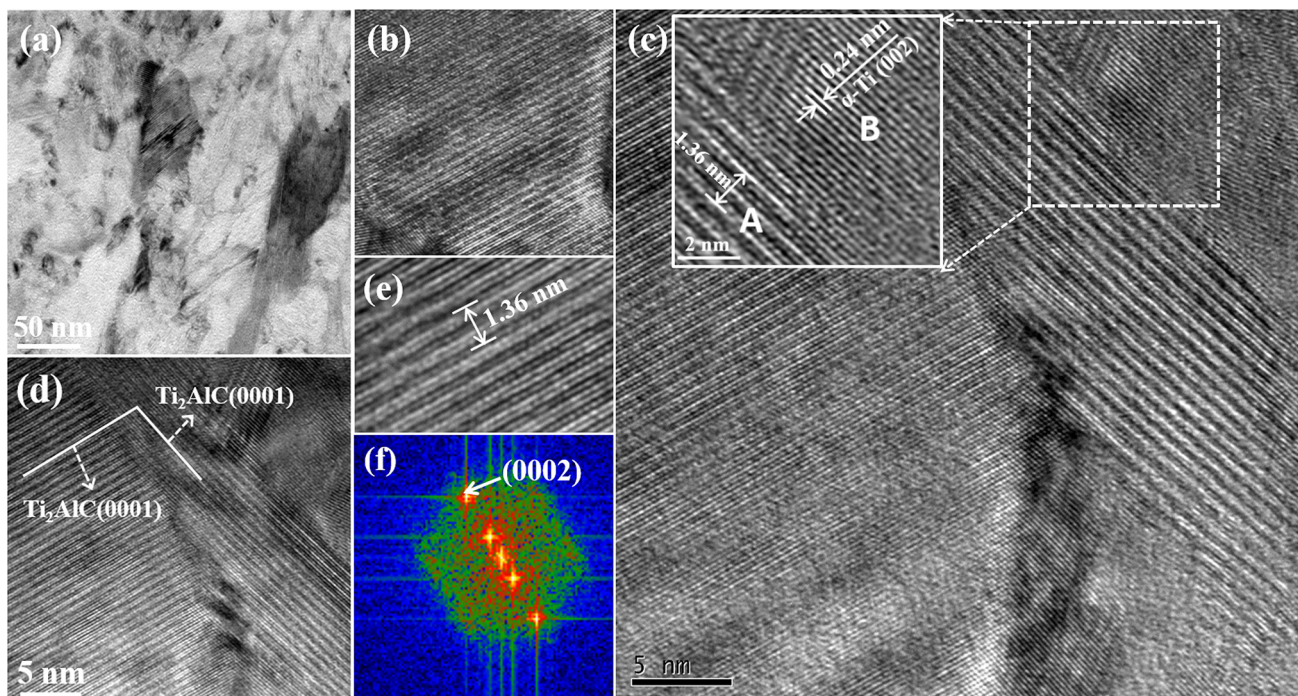


Fig. 5. Microstructures of Ti-Al-C coatings after 100 h of annealing at 550 °C. (a) TEM bright-field image of the coatings at low magnification. (b, c, d, e) HRTEM images. (f) FFT images of the area in (e).

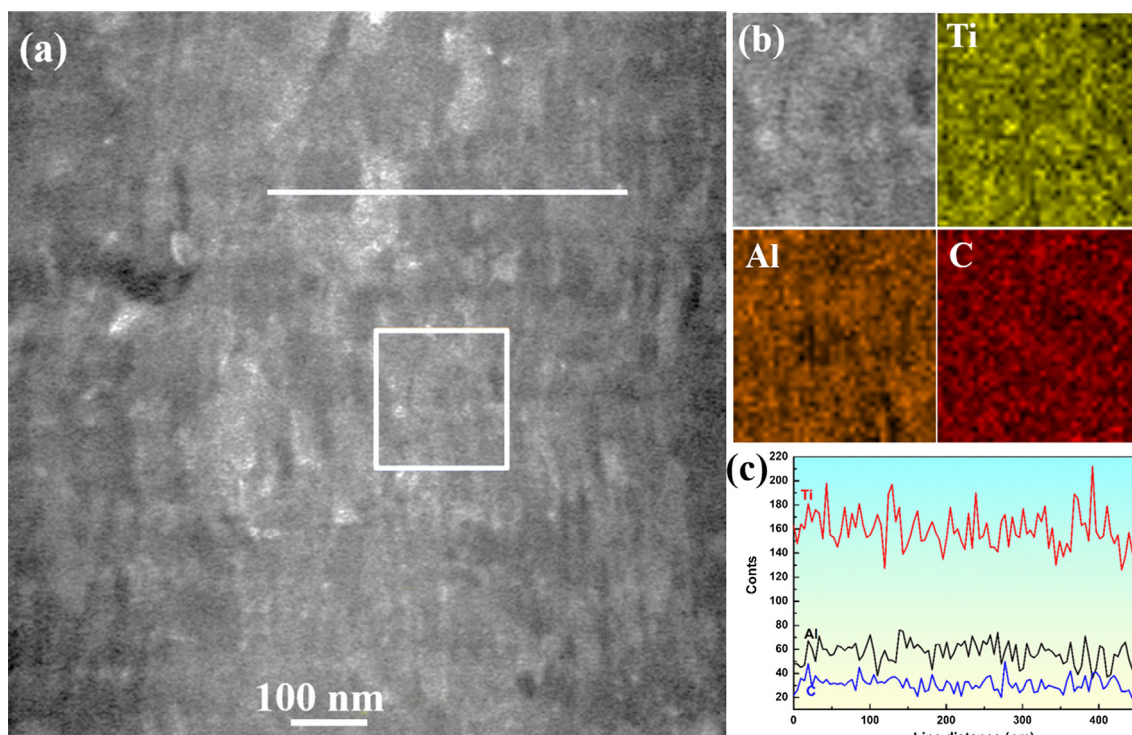


Fig. 6. (a) STEM image of the Ti-Al-C coatings after 100 h of annealing at 550 °C. (b) EDS mapping, and (c) EDS line-scanning of the yellow square area and line labeled in (a).

Ti₂AlC was considerably lower than that in the case of direct deposition from vapor phase by sputtering.

The HAADF-STEM image for the annealed coatings after 100 h of annealing at 550 °C (Fig. 6a) clearly illustrated the element diffusion behavior in contrast with the as-deposited coatings. EDS mapping results corresponding to the labeled square area and EDS line-scan profiles along the line of Fig. 6 a were shown in Fig. 6b and c. The EDS results further demonstrated that the multilayer structure disappeared after annealing and Ti, Al, and C elements distributed evenly in the annealed coatings, implying elemental diffusion during annealing.

To investigate the long-time annealing effects on the formation temperature of the Ti₂AlC MAX phase, XRD patterns of the as-deposited Ti-Al-C coatings, and the annealed ones at different annealing temperatures and time, were obtained. As shown in Fig. 7, *hcp*-TiC_{0.65} and

fcc-TiC phases were observed for the as-deposited Ti-Al-C coatings, which was in agreement with the TEM results. The Ti₂AlC MAX phases were formed after 100 h annealing at 550 °C, and their diffraction intensity improved significantly on increasing the annealing temperature to 580 °C. Unsurprisingly, the crystallinity of the Ti₂AlC phase in the Ti-Al-C coatings after 100 h annealing at 580 °C was better than that after 20 h annealing at 600 °C. In addition, the crystallinity and content of the Ti₂AlC MAX phases gradually increased on prolonging the annealing time, accompanied with the reduction of the α -TiC_{0.65} phase, which suggested that the MAX phase formation was enabled by the diffusion reaction that was dependent of annealing temperature and time. Based on the above analysis, it was concluded that the formation of Ti₂AlC MAX phases and crystalline enhancement could be achieved not only by increasing the annealing temperature but also by prolonging the annealing time at a relatively low temperature. Moreover, no other competing phases, such as intermetallic compound or carbide phases, were found in the annealed coatings in addition to a small amount of the Ti₃AlC phase appeared during annealing. The reason for this was in line with the previous report [29] that described the synthesis of polycrystalline bulk Ti₃AlC₂ via hot pressing using TiC_x ($x = 0.6$) and Al powder mixture as a starting material. This strategy made it possible to reduce the synthesis time and processing temperature, as well as increase the purity of Ti₃AlC₂. However, no Ti₂AlC MAX phase was found when the annealing temperature decreased to 500 °C even after prolonging the annealing time to 400 h. This was possibly because the diffusion activation energy was likely too low to promote the Al elements to diffuse into the TiC_x layer, which was prerequisite for the formation of the Ti₂AlC MAX phase. While there was no evidence for the formation of MAX phases from the reaction between TiC_x and Al at 500 and 600 °C in previous studies [12], as soon as Al started to diffuse into the TiC_x particles, Ti₃AlC₂ was predominantly synthesized without forming Al₃Ti as an intermediate phase.

Fig. 8 showed the TEM images of the Ti-Al-C coatings after 400 h annealing at 500 °C. The multilayer structure could be easily

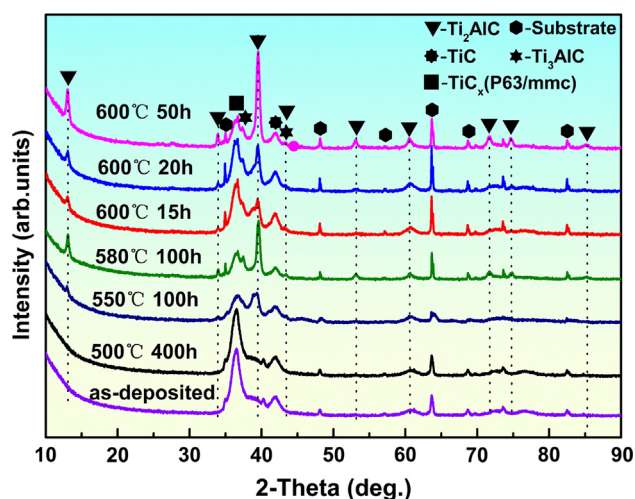


Fig. 7. XRD spectra of the as-deposited Ti-Al-C coatings and the annealed coatings at different annealing temperatures and time.

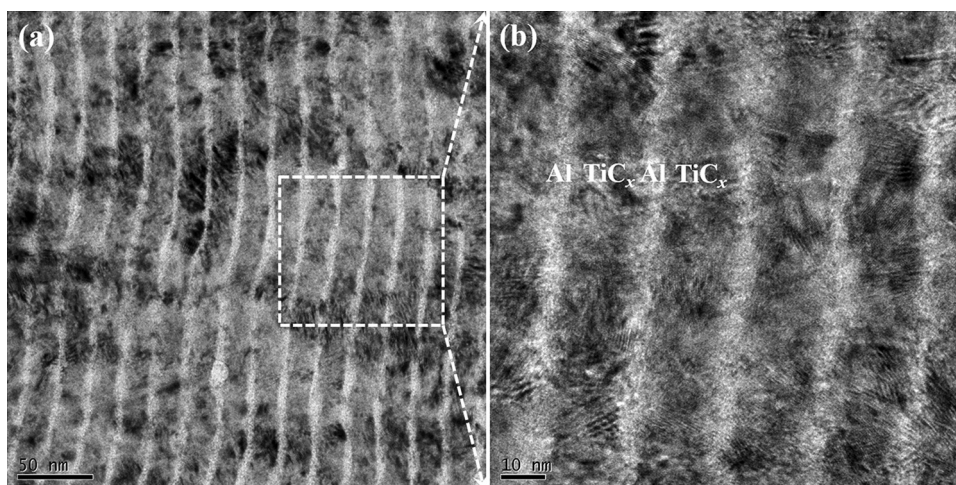


Fig. 8. Bright-field TEM image of Ti-Al-C coatings after 400 h annealing at 500 °C.

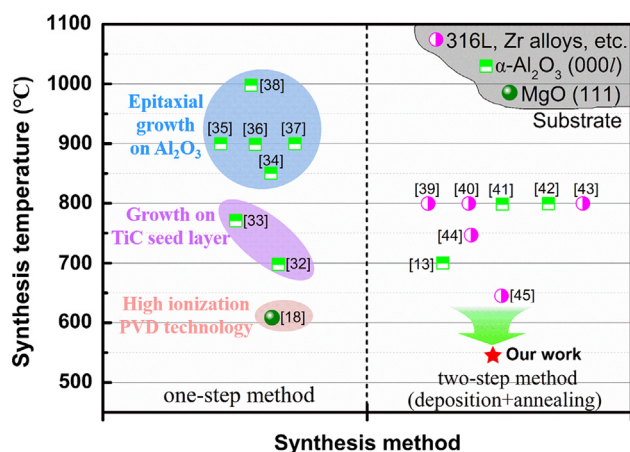


Fig. 9. Comparative results of the synthesis temperature of Ti₂AlC MAX phase coating of our work and the references.

distinguished in the TEM results, suggesting that almost no Al diffusion occurred during annealing at 500 °C because of the insufficient diffusion activation energy. Therefore, although a low-temperature synthesis pathway was designed in this study, it was not likely to form a MAX

phase for the TiC_{0.65}/Al multilayer coatings even with prolonged annealing time at the annealing temperature of 500 °C.

Previous theoretical works have demonstrated that energy required to bring order to the existing C vacancies in TiC_x ($x < 1$) was only 49 meV per vacancy, which corresponds to excitations at temperatures of ~100 °C. Subsequently, the Al element could directly diffuse into these ordered vacancy sites of TiC_x and led to the formation of the Ti₂AlC phase at low synthesis temperatures. The intercalation process could, if active, be a very promising low-temperature synthesis pathway for bulk MAX phases as well as for thin films. Experimental identification of intercalation to form bulk MAX phases has been reported in Ti₂SnC [30], Ti₃AlC₂ [31], etc. Abdulkadhim et al. [12] have provided evidence of the direct formation of Ti₂AlC by Al intercalation into TiC_x ($x \leq 0.7$) during the annealing of TiC_x(1–1.5 μm)/Al(600 nm) bilayer thin films, where the annealing temperature and holding time were 500–1000 °C and 60 min, respectively. Nevertheless, the Al diffusion-controlled intercalation process was dependent of annealing temperature and time, which directly influenced the elemental diffusion rate and length. The lower the annealing temperature, the slower the diffusion. Tang et al. have reported that elemental nano-layered coatings can achieve shorter diffusion lengths and reduce the formation temperature of the Ti₂AlC MAX phase to 600–700 °C through subsequent annealing. To achieve MAX phase synthesis at low temperature,

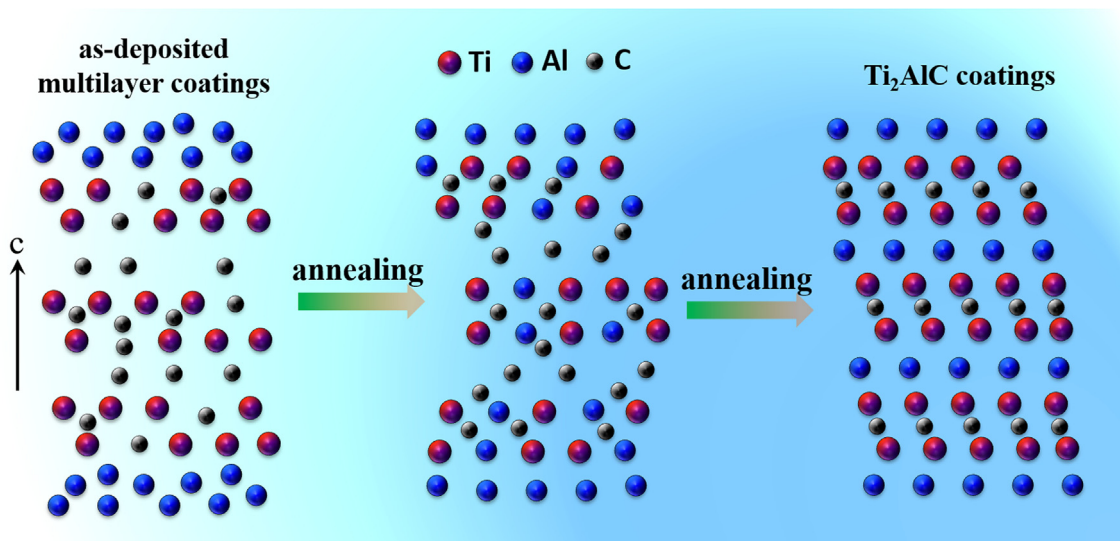


Fig. 10. Formation mechanism of Ti₂AlC coatings during annealing of the as-deposited multilayer Ti-Al-C coatings.

multilayer α -TiC_{0.65}/Al coatings were designed in our work, and long-time annealing was conducted at 500, 550, 580 and 600 °C. According to the RBS results, C vacancies (TiC_{0.65}) existed in the TiC_x layer. Unfortunately, Al elemental diffusion into the TiC_x layer was not observed when the annealing time was prolonged to 400 h at 500 °C. It was interesting to note that Ti₂AlC MAX phases formed after 100 h annealing at 550 °C, which was the lowest temperature for their synthesis reported so far (see in Fig. 9) [32–45]. In addition, HRTEM revealed that Al was directly intercalated into TiC_{0.65} to form the Ti₂AlC MAX phase. However, diffusion-controlled intercalation processes of Ti₂AlC formation were expected to be slow at low temperatures. The detailed formation mechanism of Ti₂AlC in this case was illustrated in Fig. 10, and the related mechanism also applied in other MAX phases, such as Ti₃SiC₂ [46] and Ti₂AlN [47], etc.

4. Conclusion

In summary, α -TiC_{0.65}/Al multilayer coatings were designed and prepared using the combined cathodic arc/sputter deposition system. A long-time annealing varying from 15 to 400 h was conducted for the as-deposited coatings. It was found that the Ti₂AlC MAX phases were formed at the annealing temperature of 550 °C when the annealing time was prolonged to 100 h due to the controlled sluggish diffusion kinetics. These results suggest that the synthesis temperature of MAX phases can be significantly reduced by prolonging the annealing time for the pre-designed multilayer coating, which presents a strategy to fabricate high-quality MAX phase materials at low temperature for promising wide applications.

Acknowledgements

The research was supported by the National Science and Technology Major Project (2017-VII-0012-0108), National Natural Science Foundation of China (51875555, 51901238), Chinese Postdoctoral Science Foundation (2018M632513).

References

- [1] M.W. Barsoum, The $M_{N+1}AX_n$ phases: a new class of solids; thermodynamically stable nanolaminates, *Prog. Solid St. Chem.* 28 (2000) 201–281.
- [2] N.I. Medvedeva, D.L. Novikov, A.L. Ivanovsky, M.V. Kuznetsov, A.J. Freeman, Electronic properties of Ti₃SiC₂-based solid solutions, *Phys. Rev. B* 58 (1998) 16042–16050.
- [3] B. Anasori, M.R. Lukatskaya, Y. Gogotsi, 2D metal carbides and nitrides (MXenes) for energy storage, *Nat. Rev. Mater.* 2 (2017) 16098.
- [4] F. Shahzad, M. Alhabeb, C.B. Hatter, B. Anasori, S.M. Hong, C.M. Koo, Y. Gogotsi, Electromagnetic interference shielding with 2D transition metal carbides (MXenes), *Science* 353 (2016) 1137–1140.
- [5] M. Ghidui, M.R. Lukatskaya, M.Q. Zhao, Y. Gogotsi, M.W. Barsoum, Conductive two-dimensional titanium carbide 'clay' with high volumetric capacitance, *Nature* 516 (2014) 78–81.
- [6] Q.K. Hu, D.D. Sun, Q.H. Wu, H.Y. Wang, L.B. Wang, B.Z. Liu, A.G. Zhou, J.L. He, MXene: a new family of promising hydrogen storage medium, *J. Phys. Chem. A* 117 (2013) 14253–14260.
- [7] Q. Peng, C. Si, J. Zhou, Z.M. Sun, Modulating the Schottky barriers in MoS₂/MXenes heterostructures via surface functionalization and electric field, *Appl. Surf. Sci.* 480 (2019) 199–204.
- [8] S. Aryal, R. Sakidja, M.W. Barsoum, W.-Y. Ching, A genomic approach to the stability, elastic, and electronic properties of the MAX phases, *Phys. Status Solidi B* 251 (2014) 1480–1497.
- [9] M.W. Barsoum, T. Zhen, S.R. Kalidindi, M. Radovic, A. Murugiah, Fully reversible, dislocation-based compressive deformation of Ti₃SiC₂ to 1 GPa, *Nat. Mater.* 2 (2003) 107–111.
- [10] Y. Gogotsi, A. Nikitin, H.H. Ye, W. Zhou, J.E. Fischer, B. Yi, H.C. Foley, M.W. Barsoum, Nanoporous carbide-derived carbon with tunable pore size, *Nat. Mater.* 2 (2003) 591–594.
- [11] H.-I. Yoo, M.W. Barsoum, T. El-Raghy, Materials science: Ti₃SiC₂ has negligible thermopower, *Nature* 407 (2000) 581–582.
- [12] A. Abdulkadhim, T. Takahashi, D. Music, F. Munnik, J.M. Schneider, MAX phase formation by intercalation upon annealing of TiCx/Al (0.4 ≤ x ≤ 1) bilayer thin films, *Acta Mater.* 59 (2011) 6168–6175.
- [13] H. Högborg, L. Hultman, J. Emmerlich, T. Joelsson, P. Eklund, J.M. Molina-Aldareguia, J.P. Palmquist, O. Wilhelmsson, U. Jansson, Growth and characterization of MAX-phase thin films, *Surf. Coat. Technol.* 193 (2005) 6–10.
- [14] Y.C. Zhou, Z.M. Sun, Crystallographic relations between Ti₃SiC₂ and TiC, *Mater. Res. Innov.* 3 (2000) 286–291.
- [15] D.P. Riley, E.H. Kisi, The design of crystalline precursors for the synthesis of $M_{n+1}AX_n$ phases and their application to Ti₃AlC₂, *J. Am. Ceram. Soc.* 90 (2007) 2231–2235.
- [16] A. Abdulkadhim, M.T. Baben, T. Takahashi, V. Schnabel, M. Hans, C. Polzer, P. Polcik, J.M. Schneider, Crystallization kinetics of amorphous Cr₂AlC thin films, *Surf. Coat. Technol.* 206 (2011) 599–603.
- [17] R. Shu, F.F. Ge, F.P. Meng, P. Li, J. Wang, Q. Huang, P. Eklund, F. Huang, One-step synthesis of polycrystalline V₂AlC thin films on amorphous substrates by magnetron co-sputtering, *Vacuum* 146 (2017) 106–110.
- [18] R.R. Su, H.L. Zhang, D.J. O'Connor, L.Q. Shi, X.P. Meng, H.B. Zhang, Deposition and characterization of Ti₂AlC MAX phase and Ti₃AlC thin films by magnetron sputtering, *Mater. Lett.* 179 (2016) 194–197.
- [19] L. Chen, C.R. Cao, J.A. Shi, Z. Lu, Y.T. Sun, P. Luo, L. Gu, H.Y. Bai, M.X. Pan, W.H. Wang, Fast surface dynamics of metallic glass enable superlattice-like nanostructure growth, *Phys. Rev. Lett.* 118 (2017) 016101.
- [20] A.A. Levin, D.C. Meyer, A. Gorbunov, A. Mensch, W. Pompe, P. Paufer, Phase transformations after long-time annealing in metastable Fe–Cr alloy films prepared by pulsed laser deposition, *J. Alloys Compd.* 360 (2003) 107–117.
- [21] Z.Y. Wang, J.Z. Liu, L. Wang, X.W. Li, P.L. Ke, A.Y. Wang, Dense and high-stability Ti₂AlN MAX phase coatings prepared by the combined cathodic arc/sputter technique, *Appl. Surf. Sci.* 396 (2017) 1435–1442.
- [22] Z.Y. Wang, X.W. Li, J. Zhou, P. Liu, Q. Huang, P.L. Ke, A.Y. Wang, Microstructure evolution of V–Al–C coatings synthesized from a V₂AlC compound target after vacuum annealing treatment, *J. Alloys Compd.* 661 (2016) 476–482.
- [23] P. Eklund, M. Beckers, U. Jansson, H. Högborg, L. Hultman, The $M_{n+1}AX_n$ phases: materials science and thin-film processing, *Thin Solid Films* 518 (2010) 1851–1878.
- [24] R.M. Langford, A.K. Petford-Long, Preparation of transmission electron microscopy cross-section specimens using focused ion beam milling, *J. Vac. Sci. Technol., A* 19 (2001) 2186–2193.
- [25] V. Doliqve, M. Jaouen, T. Cabioch, F. Pailloux, P. Guérin, V. Pélouin, Formation of (Ti, Al)N/Ti₂AlN multilayers after annealing of TiN/TiAl(N) multilayers deposited by ion beam sputtering, *J. Appl. Phys.* 103 (2008).
- [26] M. Bugnet, T. Cabioch, V. Mauchamp, Ph. Guérin, M. Marteau, M. Jaouen, Stability of the nitrogen-deficient Ti₂AlN_x MAX phase in Ar²⁺-irradiated (Ti,Al)N/Ti₂AlN_x multilayers, *J. Mater. Sci.* 45 (2010) 5547–5552.
- [27] R. Yu, Q. Zhan, L.L. He, Y.C. Zhou, H.Q. Ye, Si-induced twinning of TiC and formation of Ti₃SiC₂ platelets, *Acta Mater.* 50 (2002) 4127–4135.
- [28] T. Cabioch, M. Alkazaz, M.-F. Beaufort, J. Nicolai, D. Eyidi, P. Eklund, Ti₂AlN thin films synthesized by annealing of (Ti+Al)/AlN multilayers, *Mater. Res. Bull.* 80 (2016) 58–63.
- [29] J.-H. Han, S.-S. Hwang, D. Lee, S.-W. Park, Synthesis and mechanical properties of Ti₃AlC₂ by hot pressing TiCx/Al powder mixture, *J. Eur. Ceram. Soc.* 28 (2008) 979–988.
- [30] J. Zhang, B. Liu, J.Y. Wang, Y.C. Zhou, Low-temperature instability of Ti₂SnC: a combined transmission electron microscopy, differential scanning calorimetry, and x-ray diffraction investigations, *J. Mater. Res.* 24 (2012) 39–49.
- [31] C. Yang, S.Z. Jin, B.Y. Liang, S.S. Jia, Low-temperature synthesis of high-purity Ti₃AlC₂ by MA-SPS technique, *J. Eur. Ceram. Soc.* 29 (2009) 181–185.
- [32] A.V. Pshyk, E. Coy, M. Kempniński, B. Scheibe, S. Jurga, Low-temperature growth of epitaxial Ti₂AlC MAX phase thin films by low-rate layer-by-layer PVD, *Mater. Res. Lett.* 7 (2019) 244–250.
- [33] J. Frodelius, J. Lu, J. Jensen, D. Paul, L. Hultman, P. Eklund, Phase stability and initial low-temperature oxidation mechanism of Ti₂AlC thin films, *J. Eur. Ceram. Soc.* 33 (2013) 375–382.
- [34] O. Wilhelmsson, J.P. Palmquist, E. Lewin, J. Emmerlich, P. Eklund, P.O.Å. Persson, H. Högborg, S. Li, R. Ahuja, O. Eriksson, L. Hultman, U. Jansson, Deposition and characterization of ternary thin films within the Ti–Al–C system by DC magnetron sputtering, *J. Cryst. Growth* 291 (2006) 290–300.
- [35] O. Wilhelmsson, J.-P. Palmquist, T. Nyberg, U. Jansson, Deposition of Ti₂AlC and Ti₃AlC₂ epitaxial films by magnetron sputtering, *Appl. Phys. Lett.* 85 (2004) 1066.
- [36] J. Rosén, L. Ryves, P.O.Å. Persson, M.M.M. Bilek, Deposition of epitaxial Ti₂AlC thin films by pulsed cathodic arc, *J. Appl. Phys.* 101 (2007) 056101.
- [37] M.C. Guenette, M.D. Tucker, M. Ionescu, M.M.M. Bilek, D.R. McKenzie, Cathodic arc co-deposition of highly oriented hexagonal Ti and Ti₂AlC MAX phase thin films, *Thin Solid Films* 519 (2010) 766–769.
- [38] J. Frodelius, P. Eklund, M. Beckers, P.O.Å. Persson, H. Högborg, L. Hultman, Sputter deposition from a Ti₂AlC target: process characterization and conditions for growth of Ti₂AlC, *Thin Solid Films* 518 (2010) 1621–1626.
- [39] W. Garkas, C. Leyens, A. Flores-Renteria, Synthesis and characterization of Ti₂AlC and Ti₂AlN MAX phase coatings manufactured in an industrial-size coater, *Adv. Mater.* Res. 89–91 (2010) 208–213.
- [40] Z.J. Feng, P.L. Ke, A.Y. Wang, Preparation of Ti₂AlC MAX phase coating by DC magnetron sputtering deposition and vacuum heat treatment, *J. Mater. Sci. Tech.* 31 (2015) 1193–1197.
- [41] Q.M. Wang, W. Garkas, A.F. Renteria, C. Leyens, H.W. Lee, K.H. Kim, Oxidation behavior of Ti–Al–C films composed mainly of a Ti₂AlC phase, *Corros. Sci.* 53 (2011) 2948–2955.
- [42] Y. Li, G. Zhao, Y. Qian, J. Xu, M. Li, Deposition and characterization of phase-pure Ti₂AlC and Ti₃AlC₂ coatings by DC magnetron sputtering with cost-effective targets, *Vacuum* 153 (2018) 62–69.
- [43] C. Tang, M. Steinbrueck, M. Stueber, M. Grosse, X. Yu, S. Ulrich, H.J. Seifert, Deposition, characterization and high-temperature steam oxidation behavior of single-phase Ti₂AlC-coated Zircaloy-4, *Corros. Sci.* 135 (2018) 87–98.
- [44] J. Nicolai, C. Furgeaud, B.W. Fonrose, C. Bail, M.F. Beaufort, Formation

- mechanisms of Ti_2AlC MAX phase on SiC-4H using magnetron sputtering and post-annealing, *Mater. Design* 144 (2018) 209–213.
- [45] C. Tang, M. Klimenkov, U. Jaentsch, H. Leiste, M. Rinke, S. Ulrich, M. Steinbrück, H.J. Seifert, M. Stueber, Synthesis and characterization of Ti_2AlC coatings by magnetron sputtering from three elemental targets and ex-situ annealing, *Surf. Coat. Technol.* 309 (2017) 445–455.
- [46] V. Vishnyakov, J. Lu, P. Eklund, L. Hultman, J. Colligon, Ti_3SiC_2 -formation during Ti–C–Si multilayer deposition by magnetron sputtering at 600 °C, *Vacuum* 93 (2013) 56–59.
- [47] R. Grieseler, T. Kups, M. Wilke, M. Hopfeld, P. Schaaf, Formation of Ti_2AlN nanolaminate films by multilayer-deposition and subsequent rapid thermal annealing, *Mater. Lett.* 82 (2012) 74–77.